CHANDRA
X-ray Center 60 Garden St., Cambridge Massachusetts 02138 USA

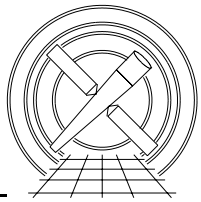

MEMORANDUM

Date: November 13, 2002
From: Christopher Allen, Diab Jerius
Subject: The Chandra Off-Axis Point Spread Function
File: `offaxis_psf.tex`
Version: `1.0`

Abstract

We present metrics for the Chandra off-axis PSF, generated using the official Chandra mirror model, SAOsac. We describe the PSF with elliptical isophotes fitted in IRAF containing particular fractions of the total beam energy. The metrics characterize the PSF in terms of the ellipses' semi-major axes and rotation angle, and cover a range of monochromatic energies between 0.277 keV and 8 keV and a spatial grid of off-axis positions which covers the focal surface. We present the results for the HRC-I detector.

Introduction

A simple parameterization of the shape and extent of the *Chandra X-ray Observatory* point spread function (PSF) at off axis angles would be a useful tool to help users analyze off-axis sources in the Chandra field, due to the fact that *CXO* off-axis point sources are heavily distorted. In addition, this characterization would increase the utility of data-mining the *CXO* archive data for sources of interest that happen to be serendipitously captured at large off-axis angles in existing observations of other sources, but are at large off-axis angles. Knowledge of the expected shape and extent of the PSF would assist users in better excluding background regions and extracting flux from the region in which the PSF is measurable. An erroneous estimate of the size of the PSF would lead to errors in the deduced source flux, temperature, spectral parameters, *etc*, limiting the data that can be extracted from off-axis sources.

We present a simple parameterization of the *CXO* off-axis PSF as sets of fitted isophotal ellipses, an improvement over the previously presented circular models. We also present encircled energy fraction (EE, the fraction of the total source energy that falls inside a given region, in our case, an ellipses) vs distance-from-PSF-center (R) and ellipse semi-major axis (SMA) vs off-axis angle results determined from these ellipses. In addition, we suggest several methods of increasing the accuracy of the elliptical fits, which we will present in the future.

Technique

Raytraces for seven monochromatic energies and six off-axis angles were generated using the SAOSAC simulation software. Ghost rays were suppressed, and the positions where the rays hit the detector were not pixelized, to boost the accuracy of the fitted ellipses. An azimuthal angle of $\phi = 0$ degrees was chosen for an initial parameterization; additional azimuthal angle data will be presented shortly.

New software was developed to model the HRC-I detector. The software's HRC-I model includes detector geometry, energy response, and pixel resolution, and simulates an aspect solution blur. Detector

geometry and energy response were modeled using the *CXC Optics Group* programs *deticpt* and *quef*, respectively.

FITS images were extracted in a 20 mm x 20 mm square ($\sim 400'$ square) around the aimpoint of the beam for each energy and off-axis angle. The images' pixel sizes were chosen empirically to ensure good spatial resolution coverage of the PSF and to optimize the elliptical isophote fitting (see below). Our selected binning sizes ranged from 1/8 $'$ to 2 $'$, and generally increased with off-axis angle.

Elliptical isophotes were fitted to the images using the IRAF *ellipse* task. The resulting elliptical fit parameters were used to create two representations of the off-axis PSF: a) EE vs R, and b) fitted ellipse SMA vs the off-axis angle of the source (see below).

Results and Problems

As off-axis angle increases, the PSF becomes much less elliptical in the core. The inner cusps, which rotate as a function of twice the azimuthal angle (as opposed to the overall PSF, which rotates as a function of the azimuthal angle), become increasingly bar-like with off-axis angle. This greatly increases the difficulty of performing meaningful isophotal fits at high off-axis angles (see Figure 1).

The isophotal ellipses that were fitted at these angles tended to converge on the bright, bar-like cusps, resulting in unrealistically high ellipticities (defined as e = 1 - b/a, where a and b are the semi-major and semi-minor axes, respectively; therefore, an ellipse with e = 0 is a circle). These unrealistically high-ellipticity ellipses have a very small area ($A_{ellipse} = \pi ab = \pi a^2(1-e)$, so for a given a, $A_{ellipse} \propto e$), and thus have a strongly lowered encircled energy, since a spatial region of the image containing a significant number of pixels with non-negligible (but relatively low surface brightness) values was excluded. This manifested itself as an incorrect, discontinuous jump in the encircled energy fraction vs R plots, as well as large jumps in ellipse position angle and ellipticity between fitted elliptical isophotes with negligibly different semi-major axes (Figures 2 and 3).

Perversely, the fitted ellipses in these situations would occasionally fit the low surface brightness region that lies at a right-angle to the inner cusps, producing a similar large jump in the in the position angle and ellipticity data, lying at 90 degrees to the above unrealistic set of fits.

To circumvent this difficulty, on the data sets in which the problem occurred the ellipticities from the smallest isophotal ellipses with good fits were used as the initial ellipticity guess, and fitting on the ellipticity parameter was disallowed. Fitting was done only on position angle and centroid for the ellipses with smaller semi-major axes. In a few cases, this resulted in a small number of ellipses rotating 90 deg and attempting to fit the low surface brightness region mentioned above, causing more discontinuous jumps in position angle; in these cases, the position angle of the elliptical isophote was also frozen, and fitting only in centroid was performed. This is essentially picking a reasonable frozen elliptical aperture and varying the semi-major axis to extract encircled energies. Examples of fitted ellipses are presented in Figures 4-7. The plots derived from the fitted ellipses (EE vs R and SMA vs off-axis source angle) are presented in Figures 8 and 9. These figures are not official data products and should not be used for any type of *Chandra* data analysis whatsoever.

We plan to fit isophotes to the image after its logarithm has been taken in the future, since the PSF images appear more elliptical in the core when viewed in log data space (see Figure 1). We are also investigating an ellipse-fitting method which uses an analysis of the images moments ($m_{pq} =$

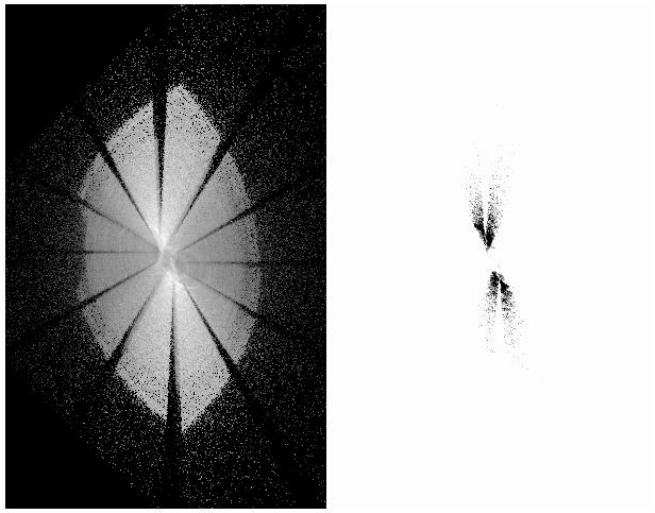

Figure 1: A side-by-side comparison of the log-scaled (left) and linear-scaled (right) 8.000 keV, 20 arcminute off-axis image highlights the non-ellipticity of the core feature.

$\sum_x \sum_y g(x,y)x^p y^q$, where m_{pq} is the p-qth moment and $g(x,y)$ is the value of a pixel at (x,y)) to produce a fitted ellipse.

Conclusion

This memo is a progress report, but we are able to draw a conclusion about the techniques used. The Chandra PSF function does not appear to be elliptical enough at large off-axis angles to use isophotal ellipses to describe it, even with careful selection of intial fitting parameters and image binning. Other techniques based on moment analysis or transforming the data into logarithm space may yield more useful results.

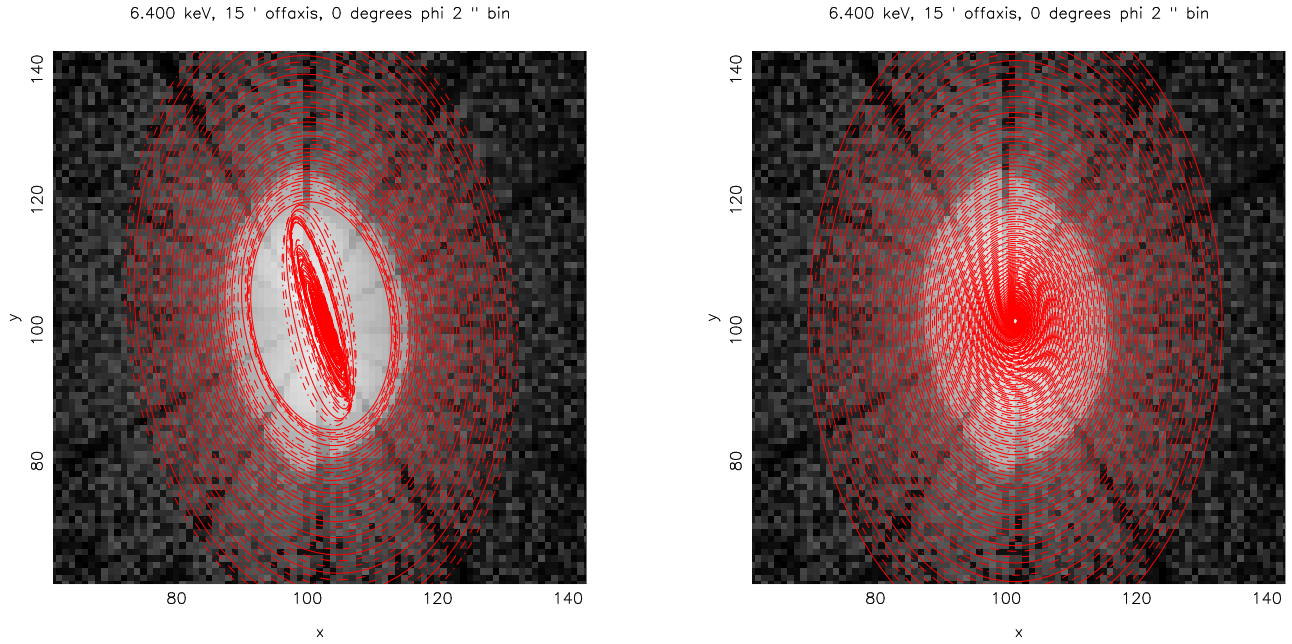

Figure 2: Left: A set of bad isophotal elliptical fits. The fit has become stuck on the core's central cusp feature, and is fitting unrealistic ellipses. Right: Selecting the ellipticity and position angle from the largest good ellipse and freezing those parameters results in a more realistic, if more rigid, set of fits.

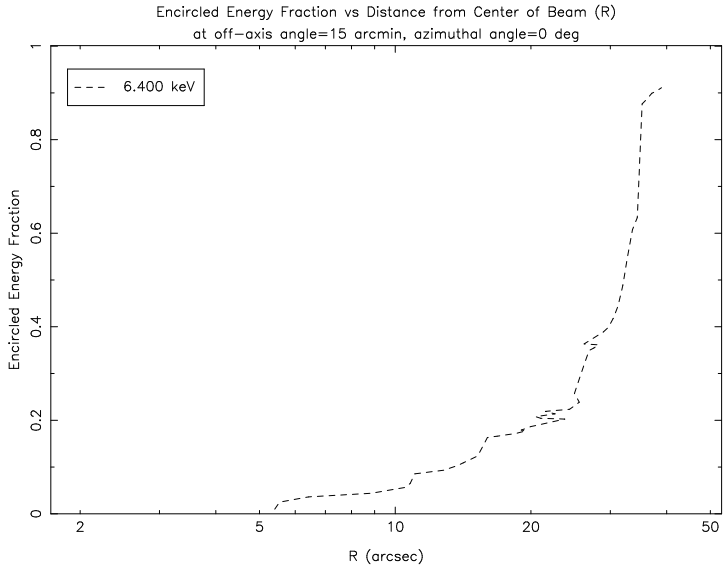

Figure 3: The horizontal jaggedness in this EE vs R plot is caused by the bad fitting in the left pane of Figure 2.

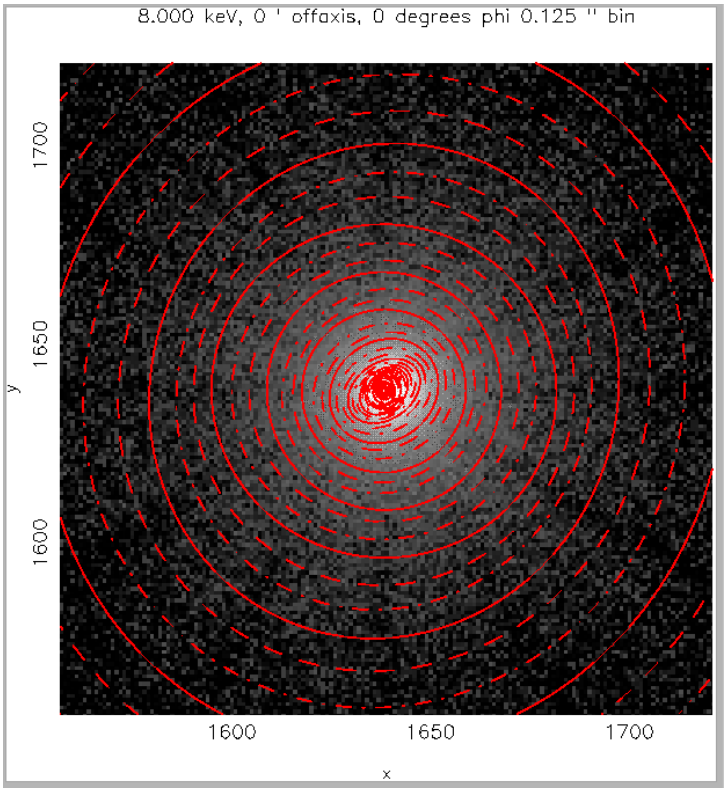

Figure 4: An on-axis PSF and its fitted ellipses. 8.000 keV.

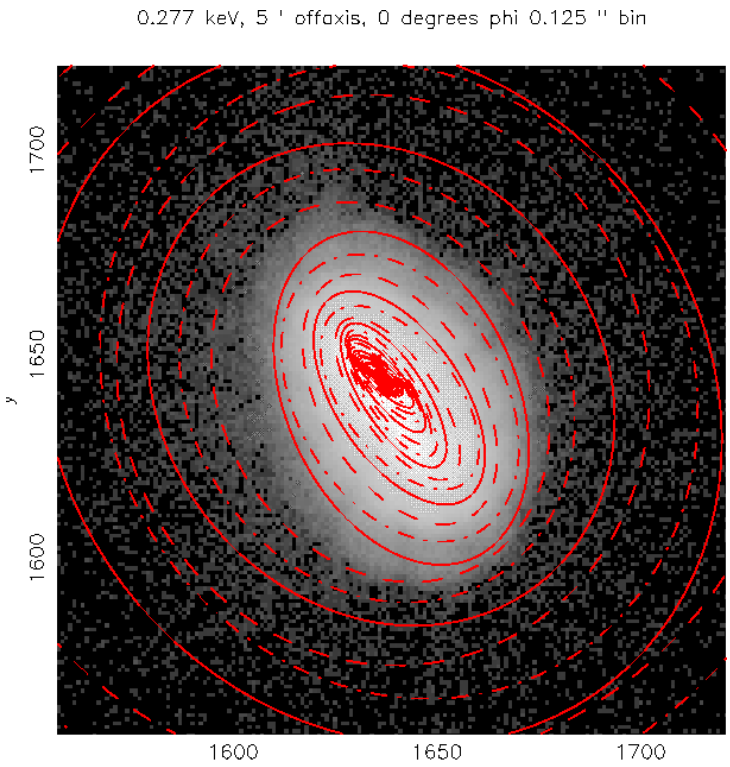

Figure 5: A typical set of fits from a 5 arcminute off-axis point source produces a PSF that is more elliptical in the core; ellipticity and position angle were fit in the above plot. 0.277 keV.

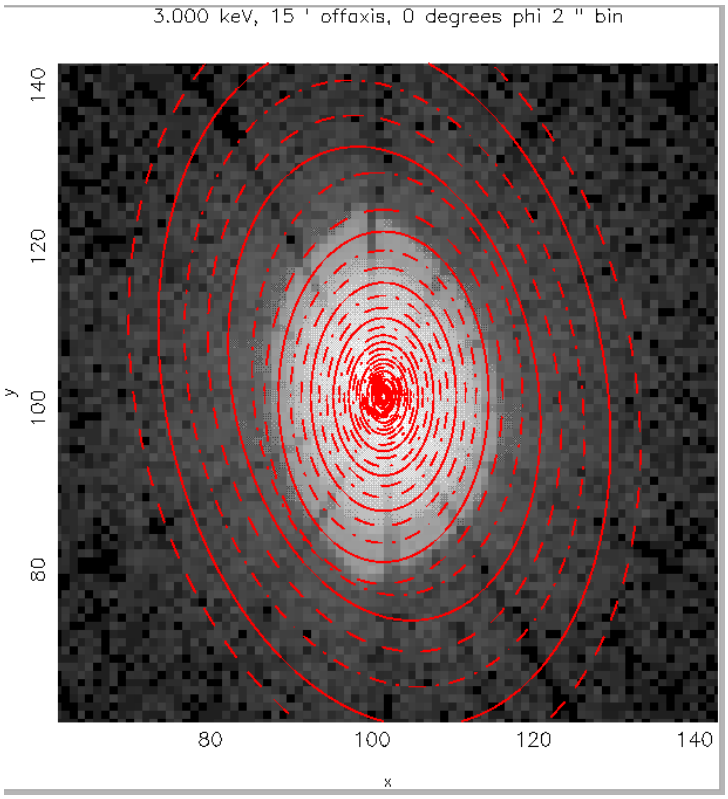

Figure 6: An example of a set of fits where ellipticity was frozen, but position angle was allowed to fit. 3.000 keV, 15 arcminutes off-axis.

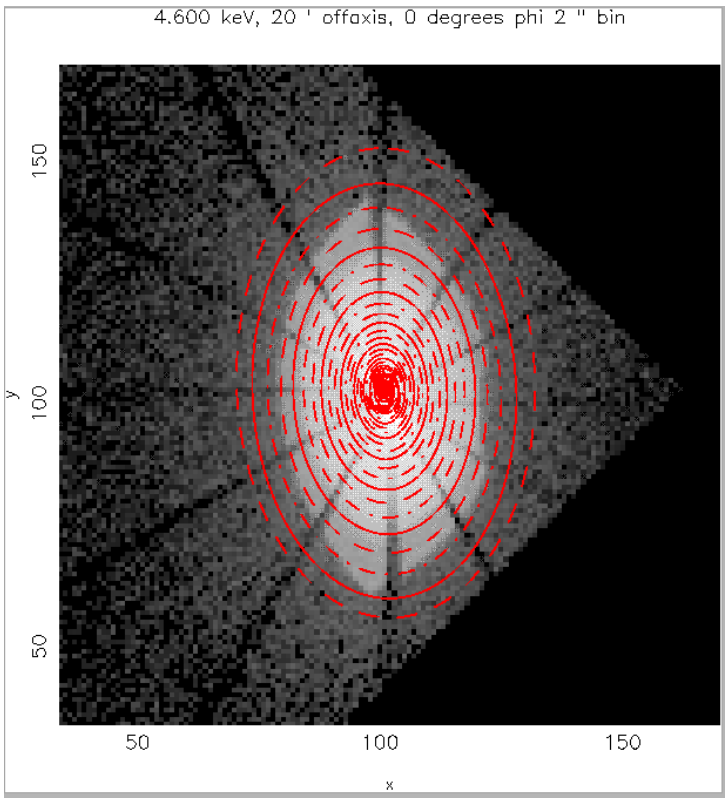

Figure 7: The elliptical isophotes fit to 4.600 keV, 20 arcminutes off-axis. Note the edge of the HRC-I cutting off the field of view. Ellipticity and position angle were frozen for this fitting.

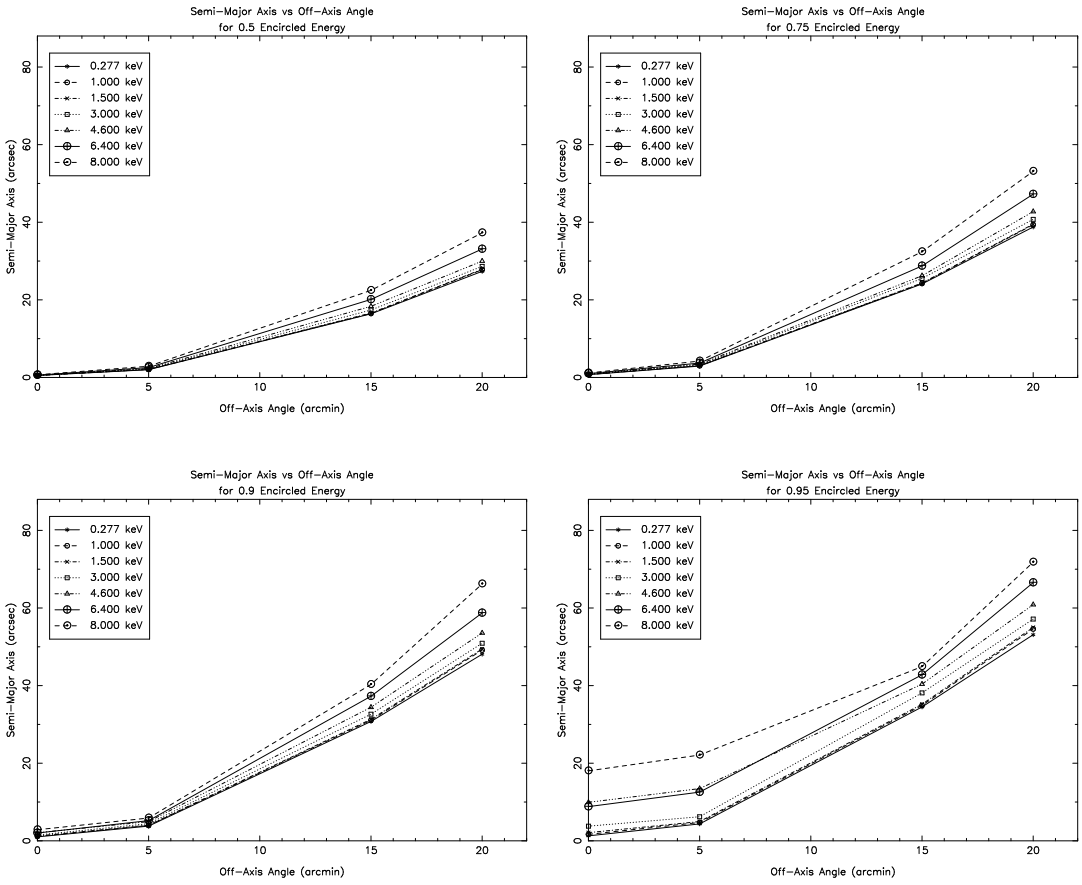

Figure 8: Semi-major axis vs off-axis angle for 0.5, 0.75, 0.90, and 0.95 encircled energy fractions. This figure is not an official data product, and should not be used for any kind of data analysis whatsoever.

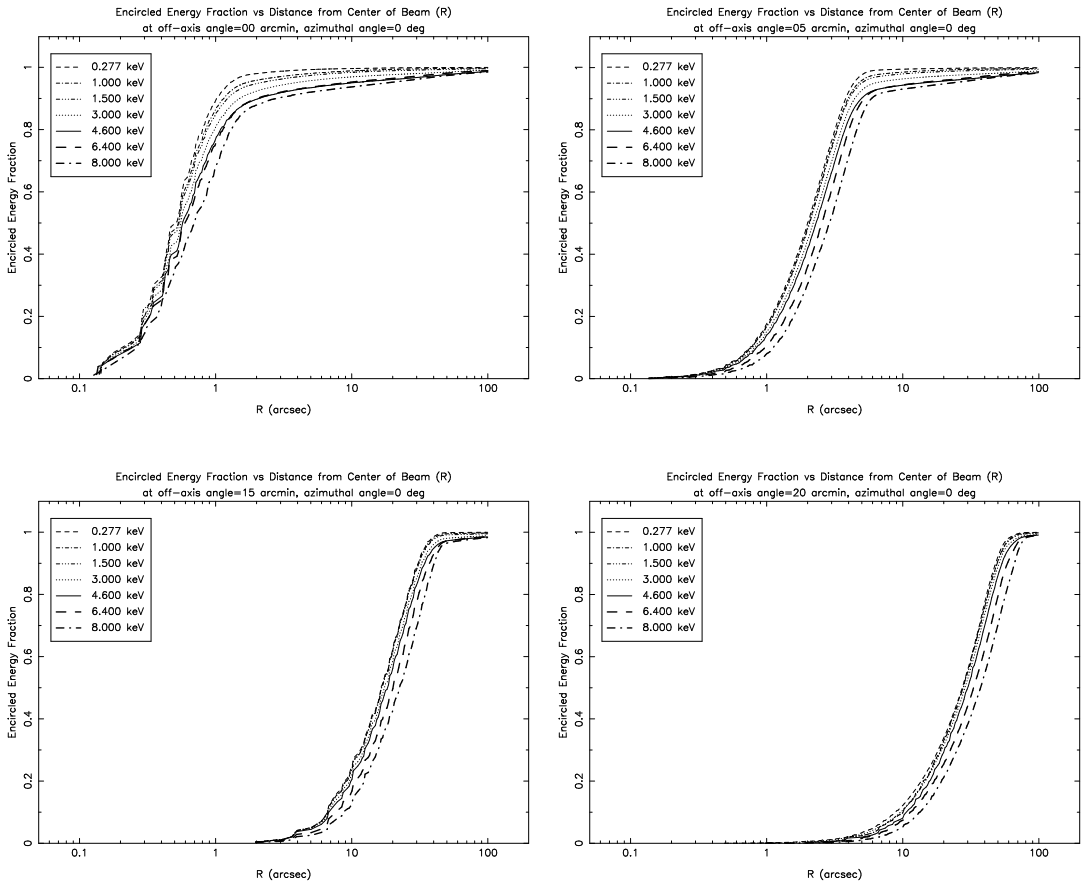

Figure 9: Encircled Energy fraction vs R (distance from center of PSF), for off-axis angles of 0, 5, 15, and 20 arcminutes. This figure is not an official data product, and should not be used for any kind of data analysis whatsoever.